

---

# Fuel-cell ejector heat pump integrated system for annual air conditioning

Renato Lazzarin, Marco Noro and Lorenzo Zamboni

*Department of Management and Engineering, University of Padova, Stradella S. Nicola, 3 – 36100, Vicenza, Italy*

**Abstract** Nowadays the need for energy produced by environmental friendly means has been leading the energy sector to more technological solutions such as fuel cells. Fuel cells generate power and reject heat through the consumption of natural gas (or hydrogen in a long term view) suitable for electrical and thermal requests for different users. The chemical process which takes place is, in principle, with no pollutants and noiseless. On the other hand, ejector heat pumps are supposed to work with low-temperature thermal energy and a limited contribution of mechanical energy thus allowing small-size heat pumps to recover fuel cells, rejected heat. The aim of this paper is to analyse the performance of the fuel-cell ejector heat pump integrated system under different conditions (at the boiler, condenser and evaporator level) and for several refrigerants, above all those with low or null ODP. A dedicated-software has been developed to undertake the energy analysis for a housing application.

**Keywords** fuel cell; ejector; heat pump

## 1. The integrated system

What we have got here is a fuel cell power supplier which is integrated with an ejector heat pump (FCHP, Fuel Cell Heat Pump) in order to supply both electrical energy and thermal energy (for housing air conditioning). The fuel cell, working with hydrogen or methane with external reformer, generates electricity (AC mode using an inverter) and heat (Figure 1).

Heat is recovered through suitable exchangers: firstly as the heat source for the heat pump boiler ( $Q_b$ ), then it is put through an air-to-air heat exchanger to directly heat the ambient air ( $Q_{ex}$ ) and finally to the evaporator<sup>1</sup> (this solution works in heating mode only; in cooling mode only  $Q_b$  is used). Heat pump follows a reversed cycle without a mechanical compression; the increase of refrigerant pressure is obtained ‘thermally’ into the ejector component. The model inputs are as follows:

- global inputs (electric and heat load profiles);
- fuel cell inputs (single cell area, cell number per stack, gases inlet pressure, etc);

---

<sup>1</sup> This solution leads to (1) higher evaporator temperatures and (2) to the independence of the system from the outside conditions during heating seasons (Autumn, Winter, Spring) and, as a consequence, to a better control of parameters.



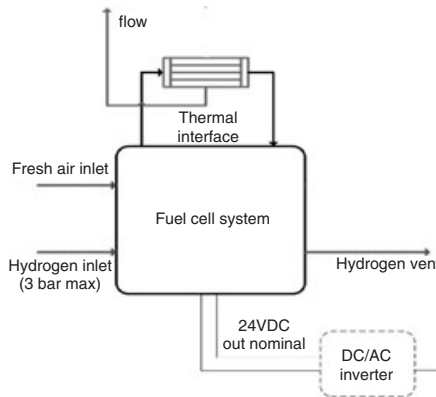
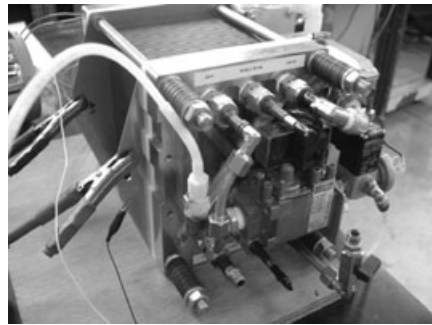


Figure 2. PEM stack (above) and co-generator fuel cell system (below) as considered in the present paper (courtesy CercoProfil S.r.l.)

Table I. Simulation data

Variables	Simulation data
Cells Number	48
H <sub>2</sub> lambda	1
Air lambda	2
Fuel	CH <sub>4</sub>
Hydrogen pressure	0.5–1 bar(g)
Air pressure	0–0.3 bar(g)
Environment air temperature	20° C
Electrode area	200 cm <sup>2</sup>

### 3. Ejector heat pump

The reference cycle is depicted in Figure 3 ([8, 9, 10]). It is possible to depict 2 cycles: a ‘power-subcycle’ (1-2-3-4-5-6-1) and the reversed cycle properly said (8-9-10-3-4-5-7-8).

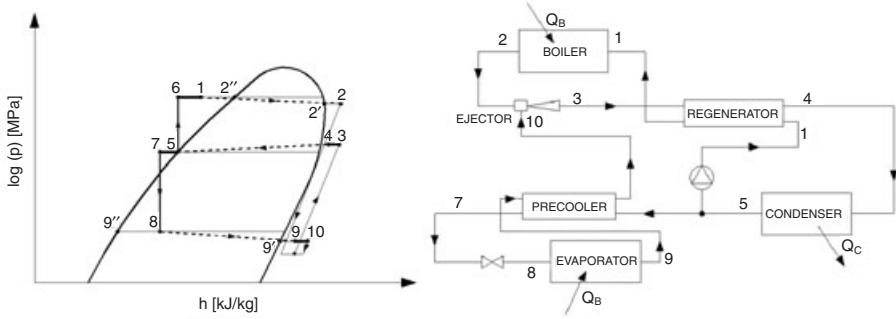


Figure 3. Ejector heat pump thermodynamic cycle diagram (left) and scheme (right).

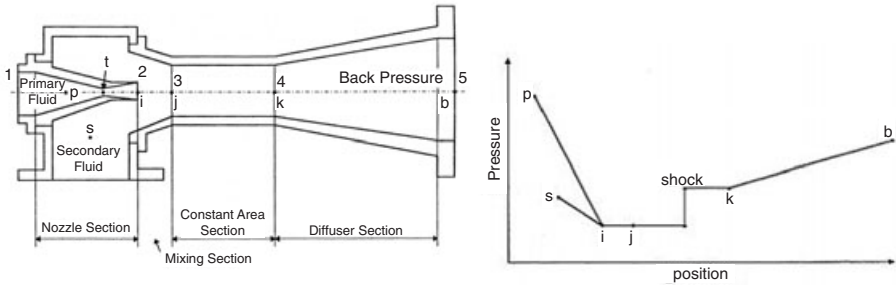


Figure 4. Ejector section and pressure diagram.

Basically, it works as follows: heat flow  $Q_B$  is concentrated to the boiler exchanger causing the heat pump refrigerant on the other side of the exchanger to get more hot (1–2''), to evaporate (2''–2') and to superheat (2'–2); such a vapour rate at high pressure (called primary flow rate,  $\dot{m}_p$ ) flows through the convergent-divergent primary nozzle into the ejector, decreasing in pressure and increasing velocity (typically to supersonic velocities) and considering approximately fulfilled the assumption of adiabatic process. The increased velocity and the low pressure downstream the primary nozzle (Figure 4) bring the refrigerant at the evaporator outlet (secondary flow rate,  $\dot{m}_s$ , see Figure 3 state 10) to be sucked when evaporator pressure is higher than primary flow pressure. Therefore, flows mix together in the *i-j* section, showing a pressure increase in section *j-k-b* (see [7] for more details about how to model the ejector). The mixture at state 3 (here pressure is supposed to be higher than condenser pressure) enters the condenser (unless it transfers heat into the regenerator in order to pre-heat the refrigerant at the boiler inlet), where it releases  $Q_c$  heat (useful in heat pump mode). At the outlet of the condenser, part of the condensate (state 5) is pumped to the boiler inlet (state 6) so closing the power-subcycle. What is left follows the reversed cycle as usual: after a subcooling process (into the pre-cooler where refrigerant at 5–7 side releases heat to refrigerant at 9–10 side) the fluid is

sent through a throttling valve (7–8, isenthalpic process) to the evaporator (8–9) where the cooling effect  $Q_E$  is applied during Summertime.

Then, the vapour at the evaporator outlet is sucked into the ejector to be compressed and the all process starts again. To estimate the efficiency of the ejector heat pump, it is possible to consider the coefficient of performance (COP) thought as ratio between the useful effect ( $Q_C$  in heat pump mode,  $Q_E$  in cooling mode) and the supplied energy ( $Q_B$  coming from the fuel cell outlet air flow and  $W_{me}$  absorbed power by the pump during process 5-6):

$$COP_{heat} = \frac{Q_c}{Q_b + W_{me}} \quad COP_{ref} = \frac{Q_e}{Q_b + W_{me}}$$

Once we want to simulate the ejector reversed cycle, it is supposed to choose the boiler, condenser and evaporator temperatures besides mass flow rate. In particular:  $T_{2''}$ ,  $T_5$ ,  $T_{9''}$  where indexes refer to scheme in Figure 3 and pressure drops are accounted as percentages of the pressures at the above three temperature states. During the two-phase processes, the average temperatures are determined as follows<sup>2</sup>:

$T_{boil} = \frac{T_{2''} + T_2}{2}$     $T_{cond} = \frac{T_5 + T_{3S}}{2}$     $T_{ev} = \frac{T_{9''} + T_9}{2}$  For further details about the heat pump modelling, please see quoted literature ([7, 8, 9, 10]).

#### 4. Refrigerant selection

The first step undertaken was the selection of the more suitable fluid for this application among a variety of candidates. The sounded parameters for the contest are the environmental impact (ODP, Ozone Depletion Potential), the cycle efficiency (both COP and entrainment ratio), but also the Area ratio ( $A_r = A_e/A_b$ ) and the operative pressures<sup>3</sup>. All fluid properties are estimated making use of a suitable routine based on software REFPROP 7.0 – NIST.

In order to evaluate the behaviour of the ejector heat pump with different fluids the simulations took into account the two systems (fuel cell and ejector heat pump) separately [7]. The boiler temperature was made to increase as a ramp while holding fixed the other temperatures (–5; 0; 5; 10°C at evaporator and 30; 35; 40; 45°C at condenser for each simulation).

The behaviour of the ejector heat pump during heating seasons is considered in the above charts: they show the COP in heating mode (Figure 5), the entrainment

<sup>2</sup> The temperature  $T_{3s}$  is the temperature of the saturated dry refrigerant at pressure  $p_3$ .

<sup>3</sup> It is well known the meaning of entrainment ratio, that is, the ratio between the secondary mass flow rate (evaporator) to the primary mass flow rate (boiler); such a ratio is proportional to the COP. Speaking about  $A_r$ , it is advisable to get values as high as possible since this condition will lead to bigger dimensions of the ejector components, so helping the manufacturing of the components themselves. Pressures should be lower than possible to have the system easier to handle (process 5–6 in Figure 3).

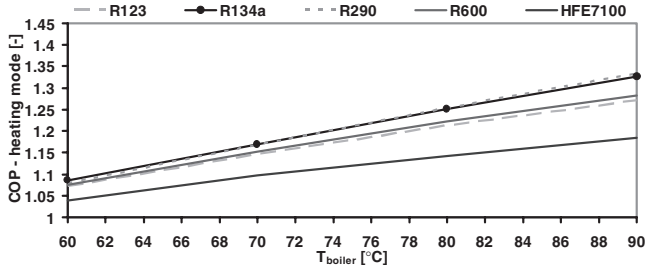


Figure 5. Coefficients of performance of fluids under study for different boiler temperatures and well known evaporator temperature ( $T_{ev} = 10^{\circ}\text{C}$ ) and condenser temperature ( $T_{cond} = 35^{\circ}\text{C}$ ).

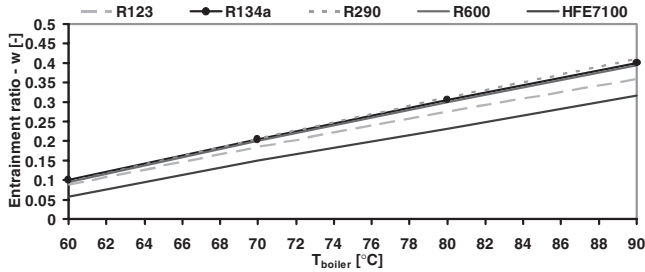


Figure 6. Entrainment ratio performances of fluids under study for different boiler temperatures and well known evaporator temperature ( $T_{ev} = 10^{\circ}\text{C}$ ) and condenser temperature ( $T_{cond} = 35^{\circ}\text{C}$ ).

ratio (Figure 6) and the area ratio (Figure 7) as function of the boiler temperature. The outcome of the model shows the optimal ejector geometry and so the best performance the system can reach for the chosen boundary conditions (temperatures, pressures, . . .). It is worth to note that not all fluids tested are plotted. Indeed, some of them do not allow the heat pump to work for the chart temperature ranges for the following reasons:

- At the outlet of the primary nozzle it is expected the presence of liquid phase (two-phase state); such a situation is merely in conflict with the assumption of one-phase flow;
- The evaporation temperature at the boiler is too close to the critical temperature for the refrigerant under study. This will cause the primary flow to get into the two-phase area as above described. A suitable superheating could solve the problem. However, this solution will not be possible for those fluids showing too low critical temperatures; on the other hand the higher the superheating the higher the temperature of the recovered heat source has to be.

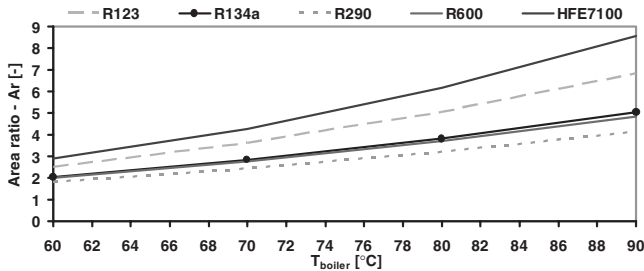


Figure 7. Area ratio performances of fluids under study for different boiler temperatures and well known evaporator temperature ( $T_{ev} = 10^{\circ}\text{C}$ ) and condenser temperature ( $T_{cond} = 35^{\circ}\text{C}$ ).

It becomes evident that:

- Simulations gives acceptable COPs: R134 gives the best results even if propane (R290) and R123 give comparable behaviours. HFE7100 shows quite low COPs, but null ODP and extremely low working pressures;
- R134a performs higher entrainment ratios than other fluids even though the ratios between the secondary mass flow rate and the primary mass flow rate for hydrocarbons and R123 are not so far from those of R134a; it is underlined that R290 and R600a are flammable and explosive;
- HFE7100 is with no doubt the fluid with the largest area ratios for the different temperature ranges (this turns in larger dimensions of the ejector and so, easier manufacturing processes leading to better efficiency of the component). It is reminded to the reader that  $A_r$  values in Figure 7 are those ones necessary to obtain the  $\varpi$  in Figure 6;
- The lowest pressures are observed only with hydrofluoroether (HFE) 7100; also R123 presents quite low operative pressures. The other fluids operate at tens of bar of pressure (also with negative effects on the pump consumption).

Consequently, R134a and HFE7100 were selected as working fluids for integrated system simulations.

## 5. Domestic application

It is simulated a semi-detached house with 2 floors; the house map is shown in Figure 8.

The building has a volume of  $302\text{ m}^3$  and its height is about 5.5 m; the ground floor has surface of  $66.4\text{ m}^2$  where the first floor has a surface of  $54.2\text{ m}^2$ . The building is thought with the main entrance to the south and, as a consequence, the kitchen and the dining room to the north. Large windows are located only in day-rooms where light is supposed to get into the house, leaving more reduced window surfaces to be placed in night-rooms and bath.



Figure 8. House map.

Table II.

	from	to	Working days	Holidays	Total days per season
Winter	07–11	31–03	104	41	145
Spring	01–04	20–05	35	15	50
Summer	21–05	17–09	86	34	120
Autumn	18–09	06–11	36	14	50

The house is split in different zones depending on characteristic temperatures and purposes. Similar zones are so grouped depending on heating or cooling needs. The family living in the house is supposed to be of 4 people: parents both working and 2 sons studying and staying out for large part of the afternoon. All cooling or heating demands all-day-long for various zones are built taking into consideration a scheduling of the thermal needs of the entire building. In particular, rooms with people are set to keep a constant temperature of 21°C in heating mode and 26°C in cooling mode, and empty rooms can not exceed, respectively, 17 °C and 30°C.

Then, it is carried out the simulation under the hypothesis of infinite heat source and sink for heating and cooling purposes, so uncoupling the wanted effects (to supply heat or to remove heat) from the chosen means (a more traditional system with radiators rather than radiant panels and so on). This is the way followed by software *Trnsys* to estimate the house thermal needs to keep indoor temperature to the set points (climate data refers to the city of Vicenza). In such a manner, eight heat load profiles are assembled and differentiated as function of the season and of the type of the day as shown in Table II. Electrical load profiles come from the data supplied by a partner of the European Project to which this paper refers to. The fuel cell-ejector heat pump integrated system brings the following points:

- study of the behaviour of the system under two different modes:
  - [a]. the system turns on when there is a thermal load to be fulfilled but it works producing electrical power to cover the requested electrical load;



- [b]. the system turns on when there is a thermal load to be fulfilled but it works producing more electrical power than needed (applying a suitable coefficient) to match the daily electrical energy demand with the daily electrical energy production. The main idea is to reduce as much as possible the consumption of electrical energy coming from the grid, but making a more intensive use of the co-generator system. Then, the electrical energy surplus is direct into the local grid since the assumption is to have the net electrical energy consumed (simply getting the difference between the energy put into the grid and the energy got from the grid)<sup>4</sup> to be paid.
- evaluation of the integrated system for two different boiler temperatures, that is: 60°C and 70°C. The lower temperature is said to be the ‘worse’ working condition whereas the other one is said to be the ‘better’ working condition. The waste heat from the fuel cell at the boiler inlet is about 80°C. The condenser temperature is set to 35°C and the evaporator temperature is set to 10°C both constant along all the heat pump work in heating mode (autumn, winter, spring). Indeed the boiler outlet air is put through the air-to-air heat exchanger and then through the evaporator so allowing a higher evaporator temperature<sup>5</sup>. During the summer the fuel cell works with an evaporation temperature of 10°C and a condenser temperature quite low around 30°C; such a low condenser temperature has to be achieved by means of a suitable heat sink.
  - comparison between the ‘innovative’ solution (*fuel cells-ejector heat pump cogenerator*) and a more ‘traditional’ solution for building air-conditioning. In particular, it is thought to use a hot water boiler working with methane (global average seasonal efficiency of 80%) and taking into account a 39% efficiency for the electrical production from power station.
  - need to handle with highly pure hydrogen because of the type of simulated fuel cell (PEM working at low temperature). Actually, apart from availability of pure hydrogen, during simulations it was considered the presence of a steam reforming for conversion of methane (CH<sub>4</sub>) to hydrogen and carbon dioxide (CO<sub>2</sub>) with an efficiency of 80%.

Figure 9–Figure 11 show the energetic comparison between the two solutions above described whereas Figure 12 shows some environmental impact considerations and lastly in the text some general economic evaluations. All figures and charts only refer to refrigerant R134a. In terms of energy saving, it is calculated the IRE index as suggested by the Italian Authority [1]:

$$IRE = 1 - \frac{E_c}{\frac{E_e}{\eta_{es} \cdot p} + \frac{E_t}{\eta_t}}$$

<sup>4</sup> It has been referred to an Italian law which allows such a behaviour for photovoltaic plants of nominal power less than 20kW.

<sup>5</sup> For sake of clarity, it has to be said that the use of heat pump in heating mode only can be rightly compared to the installation of heat exchanger directly heating the ambient air.

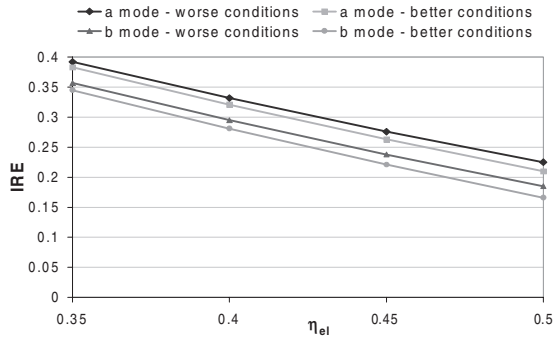


Figure 9. Energy Saving Index (IRE) vs global electric efficiency referred to stand-alone energy production.

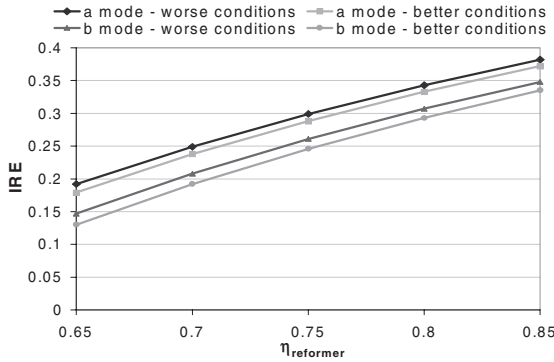


Figure 10. Energy Saving Index (IRE) vs methane-to-hydrogen conversion efficiency through steam reforming.

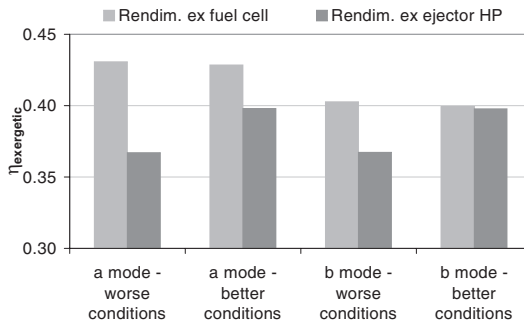


Figure 11. Exergetic efficiency for all analysed solutions.

where  $E_c$  is the fuel energy consumed during the co-generation of the electrical energy  $E_e$  and the thermal energy  $E_t$  (specifically such a thermal energy is the heat supplied by the condenser of the heat pump ( $Q_c$ ) and the heat released to the space by the air-to-air exchanger ( $Q_{ex}$ ) for heating purposes during the three seasons already mentioned). On the other hand,  $\eta_{es} = 39\%$  and  $\eta_t = 80\%$ , reflect the annual global average electrical and thermal efficiencies of the stand-alone production;  $p$  (set to 93.5%) is a coefficient accounting for transport and conversion losses not suffered by co-generative systems when consuming electrical energy they produce.

The energetic savings brought by the innovative system are quite interesting when considering today Italian scenario with an old and mainly thermo-electric system of power stations. Moreover, 'a mode' solution is supposed to perform slightly better than 'b mode' under the same heat pump conditions as depicted in Figure 10. However, in a mid-long-term the index IRE would be less interesting when considering a system of power stations working with combined-gas cycles (global average annual efficiencies around 50%). Again, increasing the methane-hydrogen conversion efficiency will result in a higher IRE index: so, no doubt about the advantage in a long-term point of view to produce hydrogen in large and centralized plants (which allow high efficiencies around 80%), even if in a mid-term scenario a localized production through small size reformers (and consequently with lower efficiencies) would show lower IRE. Figure 11 presents the exergetic efficiencies of the fuel cell and of the ejector heat pump based on the well known equations below:

$$\eta_{ex \text{ FuelCell}} = \frac{E_{el} + (Q_c + Q_{ex}) \cdot \left(1 - \frac{T_0}{T_a}\right)}{\dot{m}_{CH_4} \cdot PCI_{CH_4}}$$

$$\eta_{ex \text{ Ejector HP}} = \frac{Q_c \cdot \left(1 - \frac{T_0}{T_c}\right)}{Q_b \cdot \left(1 - \frac{T_0}{T_a}\right)}$$

where  $Q_{ex}$  is the heat released to the ambient through the air-to-air heat exchanger,  $T_a$  is a convenient mean temperature between the air temperature at the fuel cell cathode outlet and the temperature of the exhausted air,  $T_0$  is the environmental temperature (20°C) and  $T_c$  is the temperature at the condenser. The results are encouraging from the energy conversion quality point of view; for sake of precision the exergetic efficiencies during summer (cooling mode) are supposed to be lower, but can be increased if part of the heat is used to pre-heat domestic water instead of being thrown away. It is understood that fuel cell exergetic efficiencies are quite high (basically more or less equal to those energetic efficiencies because of the electro-chemical conversion) ranging between 39% and 43%; nevertheless ejector heat pump performs higher efficiencies than hot water boiler does as described in Figure 11. As a consequence savings, in terms of primary energy, range from 0.21 to 0.27 tep/year (Figure 12), respectively for 'a mode – better conditions' and 'b mode –

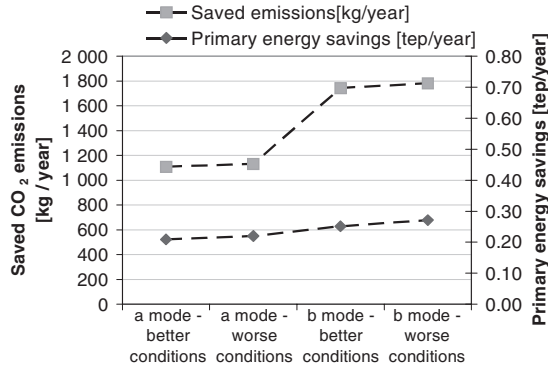


Figure 12. *Saved CO<sub>2</sub> emissions and primary energy saving when making use of the fuel cell/heat pump technology.*

worse conditions'. All charts take as a reference for comparison the stand-alone production of the electric (39% efficiency) and thermal (80% efficiency) energies.

An other important parameter which has been increasing in relevance in recent years is the production of carbon dioxide; indeed, the release of this gas into the atmosphere also contributes to the unwanted green house effect. Actually, under the assumption of local production of energy through co-generation, the integrated system allows reductions in CO<sub>2</sub> emissions from 1100 to about 1700 kg/year. It can be estimated a global decrease of the produced carbon dioxide of 5.9–9.6 Mtep/year and a primary energy saving quoted around 1–1.6 Mtep/year (about 0.7% of the global gross energy consumption in Italy during 2001 of about 188 Mtep) if it is thought one fourth of the 21 500.000 Italian families to have the 'innovative' system running.

## Acknowledgements

This paper is part of a research project 'Hybrid Fuel Cell / Heat Pump System (FUEL SAVE)' funded by the European Community.

## References

- [1] Autorità per l'energia elettrica ed il gas, Delibera n. 42/02, Condizioni per il riconoscimento della produzione combinata di energia elettrica e calore come cogenerazione ai sensi dell'articolo 2, comma 8, del decreto legislativo 16 marzo 1999, n. 79 (Italian Authority for electrical energy and gas, conditions for estimation of cogeneration energy production).
- [2] L. J. M. J. Blomen and M. N. Mugerwa, *Fuel Cell systems* (Plenum Press, 1993).
- [3] M. W. Ellis, *Fuel Cells for Building Applications* (Ashrae, 2002).
- [4] HFE-7100 thermodynamic data supplied by the University of Nottingham.
- [5] J. H. Hirschenhofer, D. B. Stauffer, R. R. Engleman and M. G. Klett, *Fuel Cell Handbook, Fourth Edition* (DoE, OFE, FETC, 1998).

- 
- [6] M. Noro, *Celle a combustibile. Tecnologia e possibilità applicative (Fuel Cells)* (Dario Flaccovio Editore, Palermo, 2003).
- [7] M. Noro, 'Celle a combustibile:modellizzazione ed analisi sperimentale per applicazioni nella produzione di energia e nella climatizzazione' ('Fuel cells: models and experimental applications'), Tesi di Dottorato (PhD thesis, 2003), Dottorato di Ricerca in Energetica XVI ciclo, Università degli Studi di Padova.
- [8] Sun Da-Wen, 1996, 'Variable geometry ejectors and their applications in ejector refrigeration systems', *Energy*, vol. 21, no. 10, 919–929.
- [9] Sun Da-Wen, 1999, 'Comparative study of the performance of an ejector refrigeration cycle operating with various refrigerants', *Energy Conversion & Management*, vol. 40, 873–884.
- [10] Sun Da-Wen and I. W. Eames, 'Performance characteristics of HCFC-123 ejector refrigeration cycles', *International Journal of Energy Research*, vol. **20** (1996), 871–885.